Eur. Phys. J. C 6, 343–348 (1999)
DOI 10.1007/s100529800917

THE EUROPEAN
PHYSICAL JOURNAL C

Double scattering on the nucleus in the perturbative QCD

M. Braun

Department of High Energy Physics, University of St. Petersburg, 198904 St. Petersburg, Russia

Received: 21 January 1998 / Revised version: 9 March 1998 / Published online: 3 September 1998

Abstract. In the hard pomeron model consequences are studied which follow from the recently obtained form of the diffractive amplitude for the double scattering on the nucleus and the related EMC effect at small x. It is shown that at large Q^2 to the double scattering contribution to the latter falls as $Q^{-0.6338}$ and in all probability dominates the total effect.

1 Introduction

Double scattering

1.1 The observed decrease of the nuclear structure functions at small x (the low x EMC effect) has long been a subject of extensive theoretical studies. In principle, the origin of the effect is clear: it is a result of the nuclear absorption for a hadron-like projectile. Many proposed models describe the existing data reasonably well [1–8]. They are all, by necessity, of a rather phenomenological nature, since the present data belong to the region of comparatively small $1/x$ and Q^2, where no reliable theory is applicable.

A more fundamental approach is possible within the hard (BFKL) pomeron model. Altough this model in its present form (a fixed coupling constant) does not, strictly speaking, refer to the QCD, nevertheless its predictions may be valid for the QCD provided the confinement effects are either inessential for the high-energy behaviour or are suitably parametrized by some cutoff parameters. In the framework of the hard pomeron model the EMC effect is a consequence of multiple pomeron exchanges or/and pomeron interactions. Thus its study provides an insight into the solution of the unitarization problem in the model.

In a recent publication [9] we studied the EMC effect in the approximation in which the number of pomerons is conserved and their interaction is neglected. The latter approximation follows if one takes the high colour N_c limit: the interaction between pomerons has a relative order $1/N_c^2$. As to the conservation of the number of pomerons and, in particular, absence of the contribution from the triple and multiple pomeron vertices, this can be justified for high enough Q^2. Indeed consider the contribution from the exchange of two pomerons shown in Fig. 1. The upper blob B describing the interaction of the virtual photon with the two pomerons has its own energy $\sqrt{s}_1$ and scaling variable $x_1 = Q^2/(s_1 + Q^2)$. Evidently the dominant contribution from the diagram in the figure comes from the region where the energy of the blob is much smaller than the total energy: $s_1 \ll s$. In fact one easily finds that s_1 is of the order $\exp(1/g^2 N_c)$, the latter quantity assumed to be large in the hard pomeron model. Now if Q^2 is of the same order (or larger, but much smaller than s) then the upper blob in the figure has finite x_1 and can be calculated perturbatively. (Strictly speaking it is in the DGLAP regime and its rigorous calculation requires knowledge of twist four operators. However, in the fixed coupling approximation and absence of any dimensionful parameters one is lead to pure perturbation theory). In the lowest approximation one finds a pair of pomerons directly coupled to the quarks in the photon. This argument seems to be valid also for a larger number of exchanged pomerons. Guided by these considerations, we summed the contributions from any number of exchanged pomerons directly coupled to the photon projectile in [9].

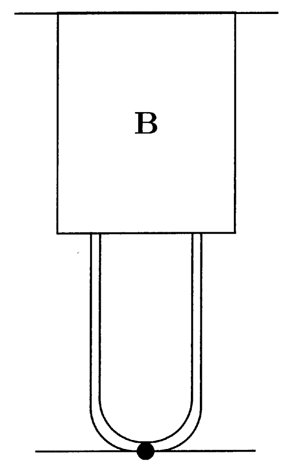

Fig. 1. A generic double pomeron exchange diagram for the scattering amplitude

What is the characteristic value Q_0^2 which marks the beginning of the applicability of the picture studied in [9]? Unfortunately it is very difficult to determine it within the hard pomeron model itself. Indeed, neither the scale of Q^2 nor the exact value of the expansion parameter of the model are well defined. If one measures Q in GeV/c and takes the pomeron intercept (minus one) Δ as the expansion parameter, then from the experimental value for the latter about 0.3 one gets $Q_0^2 \sim 30$ (GeV/c)^2. However changing the expansion parameter for a more natural $\alpha_s N_c/\pi$, with the same value of Δ, one gets $Q_0^2 \sim 10^4$ (GeV/c)^2.

In the latter case, the derivation presented in [9] results to refer to very large values of Q^2. Physically more interesting Q^2 then lie below Q_0^2 so that the upper blob in the figure has a small scaling variable x_1 and can also be treated in the framework of the hard pomeron model. This possibility is considered in the present note.

Recent studies of the system of four reggeized gluons have revealed that the direct double pomeron exchange in the hard pomeron model is equivalent to a certain triple pomeron interaction (but not vice versa) and can be excluded from the amplitude altogether [10–12]. So the situation at Q^2 below Q_0^2 is in a certain case opposite to that above Q_0^2: now the direct double pomeron exchange does not exist at all and all the contribution comes from the triple pomeron interaction. This fact seems to be true also for many exchanged pomerons. At least in the colour dipole picture of A. Mueller the total contribution reduces to a sum of pomeronic fan diagrams with only a triple pomeron interaction [12]. Unfortunately, it does not look technically possible to treat this contribution for more than two exchanged pomerons. Because of that in this note we restrict ourselves only to the double scattering on the nucleus. As will be discussed, however, this contribution seems to be dominant at high Q^2 (always below Q_0^2).

We have to stress that in any case the hard pomeron model can be applied to nuclear shadowing only in the region of high enough $1/x$ and Q^2. Present experimental data do not lie in this region. So staying strictly within the model one cannot expect a good agreement with the existing data. The model can only give predictions about the behaviour of the EMC effect at larger values of $1/x$ and Q^2 than the present ones. We hope that such values (comparable to those achieved in the study of the proton structure functions) are not beyond possibilities of the experimental activity in the future.

1.2 The amplitude $\mathcal{A}_2$ corresponding to the double scattering on the nucleus and normalized according to $2\mathrm{Im}\mathcal{A} = \sigma^{\mathrm{tot}}$ is given by the well-known expression (for $A > 2$)

$$\mathcal{A}_2 = iC_A^2 \int \frac{d^2\kappa}{(2\pi)^2} F_A(\kappa) a_2(\kappa) \qquad (1)$$

Here $F_A(\kappa)$ is a two-nucleon form-factor of the nucleus:

$$F_A(\kappa) = \int d^2r_1 d^2r_2 \rho_A(r_1, r_2) \mathrm{e}^{i\kappa(r_1 - r_2)} \,, \quad \kappa_z = 0 \qquad (2)$$

where ρ_A is a two-nucleon density. If it is taken factorized (no correlation approximation) then

$$F_A(\kappa) = T_A^2(\kappa) \qquad (3)$$

where $T_A(\kappa)$ is a two-dimensional Fourier transform of the standard nuclear profile function $T_A(b)$. For the deuteron, instead of (2),

$$F_2(\kappa) = \int d^2r |\psi(r)|^2 \mathrm{e}^{i\kappa r} \,, \quad \kappa_z = 0 \qquad (4)$$

where ψ is the deuteron wave function.

The high-energy part $a_2(\kappa)$ is given by an integral

$$ia_2(\kappa) = \frac{1}{8\pi s^2} \int_0^\infty ds_1 \mathrm{Disc}_{s_1} D(s, s_1, \kappa) \qquad (5)$$

where $D(s, s_1, \kappa)$ is a diffractive amplitude for the c.m. energy squared s, diffractive mass squared s_1 and transferred momentum κ.

We recall that the eikonal (Glauber) approximation consists in taking in (5) only a contribution from the intermediate state equal to the initial projectile hadron, which gives a_2 independent of κ:

$$a_2(\kappa) = a^2 \qquad (6)$$

where a is the forward projectile-nucleon amplitude (also normalized to $2\mathrm{Im}\, a = \sigma^{\mathrm{tot}}$). Then (1) and (3) immediately lead to the well-known result

$$\mathcal{A}_2 = iC_A^2 a^2 w_2 \,, \quad w_2 = \int d^2b T_A^2(b) \qquad (7)$$

2 Triple pomeron contribution

The diffractive amplitude found in the perurbative QCD is totally given by a contribution from the triple pomeron interaction [10–14]. So the corresponding double scattering amplitude on the nucleus will have an essentially non-Glauber form.

The discontinuity entering (5) turns out to be given by

$$\begin{aligned} D_1 &\equiv \frac{1}{2i} \mathrm{Disc}_{s_1} D(s, s_1, \kappa) \\ &= \frac{\alpha_s^5}{\pi^3} N^2(N^2 - 1) \frac{s^2}{s_1} \int \prod_{i=1}^3 d^2r_i \frac{r_1^2 \nabla_1^4}{r_2^2 r_3^2} \\ &\quad \exp(-i\kappa(r_2 + r_3)/2) \phi_1(s_1, 0, r_1) \\ &\quad \phi_2(s_2, \kappa, r_2) \phi_2(s_2, -\kappa, -r_3) \\ &\quad \delta^2(r_1 + r_2 + r_3) \end{aligned} \qquad (8)$$

Here $\phi_i(s, \kappa, r)$, describe the upper ($i = 1$) and two lower pomerons ($i = 2$, see Fig. 1) for the energetic variable s, momentum κ and the intergluon transverse distance r. N is the number of colours; $s_2 = s/s_1$. The pomerons are joined by the triple pomeron vertex, whose form was obtained in [10–12, 15] in the high-colour limit. Presenting the δ-function as an integral over the auxiliary momentum q we rewrite (8) in the form

$$\begin{aligned} D_1 &= \frac{\alpha_s^5}{\pi^3} N^2(N^2 - 1) \frac{s^2}{s_1} \int \\ &\quad \frac{d^2q}{(2\pi)^2} \chi_1(s_1, 0, q, +\kappa/2) \chi_2^2(s_2, \kappa, q) \end{aligned} \qquad (9)$$

where

$$\chi_1(s,0,q) = \int d^2 r r^2 \nabla^4 \phi_1(s,0,r) \exp iqr \qquad (10)$$

and

$$\chi_2(s,\kappa,q) = \int d^2 r r^{-2} \phi_2(s,\kappa,r) \exp iqr \qquad (11)$$

The solutions $\phi_{1(2)}$ can be obtained by using the Green function of the BFKL equation for a given total momentum $G_s(\kappa, r, r')$. , For the projectile (see [3]):

$$\phi_1(s,\kappa,r) = \int d^2 r' (G_s(\kappa,r,0) - G_s(\kappa,r,r')\rho_1(r') \qquad (12)$$

Here $\rho_1(r)$ is the colour density of the projectile as a function of the intergluon distance with the colour factor $(1/2)\delta_{ab}$ and g^2 separated. In our case the projectile is a highly virtual photon with his momentum squared $-Q^2 \leq 0$, which splits into $q\bar{q}$ pairs of different flavours. The explicit form of ρ is then well-known for this case [3]. For the transverse photon

$$\rho_1^{(T)}(r) = \frac{e^2}{4\pi^3} \sum_{f=1}^{N_f} Z_f^2 \int_0^1 d\alpha \qquad (13)$$
$$(m_f^2 K_0^2(\epsilon_f r) + (\alpha^2 + (1-\alpha)^2)\epsilon_f^2 K_1^2(\epsilon_f r))$$

where $\epsilon_f^2 = Q^2\alpha(1-\alpha) + m_f^2$ and m_f and Z_f are the mass and charge of the quark of flavour f. For the longitudinal photon

$$\rho_1^{(L)}(r) = \frac{e^2}{\pi^3} Q^2 \sum_{f=1}^{N_f} Z_1^2 \int_0^1 d\alpha \alpha^2 (1-\alpha)^2 K_0^2(\epsilon_f r) \qquad (14)$$

For the hadronic target, we assume an expression similar to (12) with a colour density $\rho_2(r)$ non-perturbative and its explicit form unknown. For our purpose it is sufficient to know that the corresponding mass scale is not large.

The two lower pomerons are in their asymptotic regime. So χ_2 can be found using an asymptotic expression for the pomeron Green function, in the same way as in [16], to which paper we refer for the details. One obtains then

$$\chi_2(s,\kappa,q) = 8s^{\Delta}(\pi/\beta \ln s)^{3/2} F_2(\kappa) J(\kappa,q) \qquad (15)$$

where $\Delta = (\alpha_s N/\pi) 4 \ln 2$ is the pomeron intercept, $\beta = (\alpha_s N/\pi) 14\zeta(3)$,

$$J(\kappa,q) = \int \frac{d^2 p}{2\pi} \frac{1}{|\kappa/2 + \rho|\,|\kappa/2 - p|\,|q+p|} \qquad (16)$$

and $F_2(\kappa)$ desribes the coupling of the lower pomeron to the target

$$\int d^2 R d^2 r \frac{\exp(i\kappa R) r \rho_2(r)}{|R + r/2|\,|R - r/2|} = \pi F_2(\kappa) \qquad (17)$$

At small κ F_2 diverges logarithmically:

$$F_2 \simeq -4(R/N) \ln \kappa\,, \quad \kappa \to 0 \qquad (18)$$

where

$$R = \frac{N}{2} \int d^2 r r \rho_2(r) \qquad (19)$$

has a meaning of the average target dimension.

If one also takes an asymptotic expression for the upper pomeron then the whole discontinuity D_1 aquires a factorized form [16] corresponding to the triple pomeron contribution in the old Regge-Gribov theory:

$$D_1(s,s_1,\kappa) = -\gamma_1 \gamma_2^2(\kappa) \gamma_{3P}(\kappa) P(s_1,0) P^2(s/s_1,\kappa) \qquad (20)$$

Here $P(s,\kappa)$ is the pomeron propagator

$$P(s,\kappa) = 2\sqrt{\pi} s^{1+\Delta} (\beta \ln s)^{-\epsilon} \qquad (21)$$

with $\epsilon = 1/2(3/2)$ for $\kappa = 0(>0)$. The vertices $\gamma_{1(2)}$ describe the pomeron interaction with the projectile (target). Using (13) and (14) one obtains, neglecting the quark masses

$$\gamma_1 = \alpha_s \sqrt{N^2 - 1}(b/Q) \exp\left(-\frac{\ln^2 Q}{\beta \ln s}\right) \qquad (22)$$

where Q^2 is the photon virtuality and for a transverse (T) and longitudinal (L) photons

$$b_T = \frac{9\pi e^2 Z^2}{256}\,, \quad b_L = \frac{2}{9} b_T \qquad (23)$$

$Z^2 = \sum_f Z_f^2$. The target vertex γ_2 is proportional to F_2, (17)

$$\gamma_2(\kappa) = \alpha_s \sqrt{N^2 - 1} F_2(\kappa) \qquad (24)$$

and so logarithmically divergent at small κ. The triple pomeron coupling γ_{3P} is also singular at small κ:

$$\gamma_{3P}(\kappa) = \frac{32\alpha_s^2 N^2}{\sqrt{N^2 - 1}} \frac{B}{\kappa} \qquad (25)$$

where the number B is given by a 6-dimensional integral over auxiliary momenta [12]. Numerical calculations give

$$B = 4.98 \pm 0.01 \qquad (26)$$

in agreement with the analytic result recently obtained in [17,18] (their $g_{3P} = (2\pi)^4 B$).

Putting explicit expressions for P's and γ's into (20) and performing the integration over s_1 one finds

$$a_2 = -c_2 \frac{R^2}{Q} \frac{s^{2\Delta}}{(\beta \ln s)^3} \frac{\ln^2 \kappa}{\kappa} \qquad (27)$$

where c_2 is a known number. From this purely asymptotic expression one could come to two conclusions. First, the double scattering contribution behaves in Q exactly as the single scattering term, that is, as $1/Q$. As a result, the EMC effect related to it should be independent of Q. Of course, this is an immediate consequence of the factorization property of the asymptotic triple pomeron interaction. Second, the singularity at small κ leads to a stronger dependence on A. Since roughly speaking $\kappa \sim$

$1/R_A$ where R_A is the nuclear radius, from (27) one could conclude that the double scattering is enhanced by a factor $(R_A/R)\ln^2(R_A/R)$ as compared to the standard eikonal result.

However all these conclusions are in fact wrong, since the upper pomeron enters the triple pomeron interaction not at asymptotic energies $\alpha_s \ln s \gg 1$ but at lower ones $\alpha_s \ln s \sim 1$, where the asymptotic expression for its Green function used in (20) is not valid. So we have to recur to the exact expression for it. Due to azimuthal symmetry of the projectile colour density we can retain only terms with zero orbital momentum in it:

$$G_s(0,r,r') = (1/8)rr' \int_{-\infty}^{\infty} \frac{d\nu s^{\omega(\nu)}}{(\nu^2+1/4)^2}(r/r')^{-2i\nu} \tag{28}$$

where

$$\omega(\nu) = 2(\alpha_s N/2\pi)(\psi(1) - \mathrm{Re}\psi(1/2+i\nu)) \tag{29}$$

If we take this expression, put it into χ_1, Eq. (10) and integrate first over s_1, as indicated in (10), and afterwards over r, we obtain

$$\int ds_1 s_2^{-1-2\Delta}\chi(s_1,0,q) = -\frac{4\pi}{q}\int d^2r'r'\rho_1(r')I(q,r') \tag{30}$$

where $I(q,r')$ is the remaining integral over ν:

$$I(q,r') = \int d\nu \frac{(qr'/2)^{2i\nu}}{2\Delta - \omega(\nu)}\frac{\Gamma(1/2-i\nu)}{\Gamma(1/2+i\nu)} \tag{31}$$

The asymptotic expression discussed above follows if one takes in (31) all terms except the denominator $2\Delta - \omega(\nu)$ out of the integral at $\nu = 0$ and in the denominator presents $\omega(\nu) = \Delta - \beta\nu^2$. Evidently this procedure is wrong. In fact, the integral (31) can be calculated as a sum of residues of the integrand at points $\nu = \pm ix_k$, $0 < x_1 < x_2 < \ldots$, at which

$$2\Delta - \omega(\nu) = 0 \tag{32}$$

Residues in the upper semiplane are to be taken if $qr'/2 > 1$ and those in the lower semiplane if $qr'/2 < 1$. Thus we obtain

$$I(q,r') = \frac{2\pi^2}{\alpha_s N}\sum_k c_k^{(\pm)}(qr'/2)^{\pm 2x_k} \tag{33}$$

where

$$c_k^{(\pm)} \frac{\Gamma(1/2 \mp x_k)/\Gamma(1/2 \pm x_k)}{\psi'(1/2-x_k) - \psi'(1/2+x_k)} \tag{34}$$

and the signs should be chosen to always have $(qr'/2)^{\pm 2x_k} < 1$.

The first three roots of (32) are

$$x_1 = 0.3169\,, \quad x_2 = 1.3718\,, \quad x_3 = 2.3867 \tag{35}$$

with the corresponding coefficients $c_k^{(\pm)}$

$$\begin{aligned} &c_1^{(+)} = 0.1522\,,\ c_2^{(+)} = -0.1407\,,\ c_3^{(+)} = 0.03433\,, \\ &c_1^{(-)} = 0.007866\,,\ c_3^{(-)} = -0.001802\,,\ c_2^{(-)} = 0.004494 \end{aligned} \tag{36}$$

Returning to (5) for a_2 as an integral of the discontinuity D_1 and putting expressions for χ_2 and the integrated χ_2, (15) and (30), into the latter we obtain

$$\begin{aligned} a_2 = &-128\pi^2\alpha_s^4 N(N^2-1)\frac{s^{2\Delta}}{(\beta\ln s)^3} \\ &F_2^2(\kappa)\sum_k \int d^2r r\rho_1(r)\left[c_k^{(+)}\left(\frac{r}{2}\right)^{2x_k} B_k^{(+)}(r,\kappa)\right. \\ &\left.+c_k^{(-)}\left(\frac{r}{2}\right)^{-2x_k} B_k^{(-)}(r,\kappa)\right] \end{aligned} \tag{37}$$

where

$$\begin{aligned} B_k^{(\pm)}(r,\kappa) = &\int \frac{d^2q}{(2\pi)^2 q} q^{\pm 2x_k} \\ &J^2(\kappa, q-\kappa/2)\theta(\pm(2/r - q)) \end{aligned} \tag{38}$$

As we observe, in the general case the factorization property is lost: the integrals $B^{(\pm)}$ depend nontrivially both on the projectile and target variables. However one can see theat this property is restored in the limit of high Q^2, relevant for the hadronic structure functions. In fact, in this limit the characteristic values of r are small: $r \sim 1/Q$. Let us study how the integrals $B^{(\pm)}$ behave at small r. In $B^{(\pm)}$ evidently large values of q are essential. The integrals J behave as $\ln q/q$ at $q \to \infty$. This leads to the following behaviour.

$$\begin{aligned} &B_k^{(+)}(r,\kappa) \sim r^{1-2x_k} \text{ if } 2x_k > 1\,, \text{and } \sim \text{const if } 2x_k < 1 \\ &B_k^{(-)}(r,\kappa) \sim r^{1+2x_k} \end{aligned}$$

Combining this with other factors depending on r we see that all terms multiplying ρ_1 in the integrand behave as r^2 at small r, except the first term with $k = 1$, which, due to $2x_1 < 1$, behaves as r^{1+2x_1}. Evidently this term gives the dominant contribution in the limit $Q^2 \to \infty$, when (37) simplifies to

$$\begin{aligned} a_2 = &-2^{7-2x_1}\pi^2\alpha_s^4 N(N^2-1)c_1^{(+)} \\ &\frac{s^{2\Delta}}{(\beta\ln s)^3}F_2^2(\kappa)\frac{b_1 B_1}{Q^{1+2x_1}\kappa^{1-2x_1}} \end{aligned} \tag{39}$$

where the numbers b_1 and B_1 are very similar to our old b and B with additional powers of the variable in the integrand:

$$b_1 = Q^{1+2x_1}\int d^2r r^{1+2x_1}\rho_1(r) \tag{40}$$

(it does not depend on Q) and

$$B_1 = \kappa^{1-2x_1}\int \frac{d^2q}{(2\pi)^2 q} q^{2x_1} J^2(\kappa, q-\kappa/2) \tag{41}$$

(it does not depend on κ). Numerical calculations give

$$\begin{aligned} &b_1^{(T)} = 0.3145e^2Z^2\,, \quad b^{(L)} = 0.04377e^2Z^2\,, \\ &B_1 = 17.93 \end{aligned} \tag{42}$$

Thus in the high-Q limit the expression for a_2 fully factorizes in the projectile and target. Its dependence on Q and κ turns out to be intermediate between the eikonal and asymptotic triple pomeron predictions. It vanishes at large Q as $1/Q^{1+2x_1}$, faster than the single pomeron exchange and asymptotic triple pomeron ($\sim 1/Q$) but not so fast as the eikonal prediction $1/Q^2$. It is also singular at $\kappa \to 0$, but the singularity is weaker than predicted by the asymptotic triple pomeron.

The double scattering amplitude following from (39) is

$$\mathcal{A}_2 = iC_A^2 2^{11-2x_1}\pi^2\alpha_s^4\frac{N^2-1}{N}c_1^{(+)}\tilde{w}_2 b_1 B_1 \frac{s^{2\Delta}}{(\beta\ln s)^3}\frac{R^2}{(QR_A)^{1+2x_1}} \tag{43}$$

where with a logarithmic accuracy (see (18))

$$\tilde{w}_2 = R_A^{1+2x_1}\int\frac{d^2\kappa}{(2\pi)^2}\kappa^{-1+2x_1}F_A(\kappa)\ln^2\kappa \tag{44}$$

and we have introduced the nuclear radius R_A to make $\tilde{w}_2$ dimensionless. Passing to the low-x EMC effect we have to compare it with the dominant single scattering term

$$\mathcal{A}_1 = iC_A^1\gamma_1\gamma_2(0)P(s,0) \tag{45}$$

where, calculated at κ exactly equal to zero, $\gamma_2(0)$ is finite:

$$\gamma_2(0) = 2\alpha_s\sqrt{N^2-1}(R/N) \tag{46}$$

The EMC effect is characterised by the EMC ratio R_{EMC} of the nuclear structure function to A times the nucleon one. The double scattering contribution to it is given by $R_{EMC} = 1-\lambda_A$ where $\lambda_A = -\mathcal{A}_2/\mathcal{A}_1$. From our formulas we find

$$\lambda_A = c(A-1)\tilde{w}_2\frac{R}{R_A}\frac{1}{(QR_A)^{2x_1}} \frac{s^{\Delta}}{(\beta\ln s)^{5/2}}\exp\left(\frac{\ln^2 Q}{\beta\ln s}\right) \tag{47}$$

where the numerical coefficient is

$$c = 2^{9-2x_1}\pi^{3/2}\alpha_s^2 c_1^{(+)}B_1(b_{1T}+b_{1L})/(b_T+b_L) \tag{48}$$

From (47) we expect the EMC effect to go to zero as $Q\to\infty$ as Q^{-2x_1}, that is, rather slowly, essentially slower than one would find from the eikonal picture. Its dependence on A is enhanced by a factor $\sim (R_A/R)^{1-2x_1}\ln^2(R_A/R)$ as compared to the eikonal prediction. The enhancement is not so strong as one might naively predict on the basis of the asymptotic triple pomeron picture.

3 Some numerical estimates

The obtained formulas in principle allow to calculate the double scattering contribution to the EMC effect on nuclei at small x. Since the EMC effect is small experimentally, one may hope that this contribution practically exhausts it (also see Conclusions for some justification). Our formulas contain two parameters: the strong coupling constant α_s and the nucleon radius R. The value of α_s can be extracted from the observed intercept Δ. As to R, it has to be of the order of the proton electromagnetic radius. Of course, one has to take into account inevitable uncertainties associated with the logarithmic character of the hard pomeron model and absence of scale in $\log s$ and $\log\kappa$. However in trying to apply our formulas to the experimental situation one meets with another serious obstacle.

Comparison of the experimental proton structure function with the predictions based on the hard pomeron model indicates that the model can only be valid at very small $x \le x_0 = 0.01$. A power growth characteristic for the hard pomeron can be supported experimentally at $x \sim x_1 = 10^{-4}$–10^{-5}. The triple pomeron interaction picture requires that both s_1 for the upper pomeron and s/s_1 for the two lower ones be correspondingly large. It follows that this picture can only be applicable at extraordinary small $x \le x_0x_1 = 10^{-6}$. Besides, the large Q^2 limit used to obtain a factorizable form for the contribution requires that $(QR_A)^{1-2x_1} \gg 1$. Present experimental data on the EMC effect do not satisfy these requirements. They are restricted to $x > 0.005$ and values of Q^2 below 2 $(\mathrm{GeV}/c)^2$ for $x < 0.01$. Thus, comparison of our predictions to the existing data cannot be justified.

If, notwithstanding this objection, one takes realistic values $\Delta = 0.2$ and $R = 0.44\,\mathrm{fm}$ [9], then for Ca at $x = 0.0085$, $Q^2 = 1.4\,(\mathrm{GeV}/c)^2$ one gets $\lambda = 0.14$ in an agreement with the experimental value $\lambda^{\mathrm{ex}} = 0.154 \pm 0.014$. However with the same parameters for Xe at $x = 0.0065$, $Q^2 = 1.34\,(\mathrm{GeV}/c)^2$ and C at $x = 0.0055$, $Q^2 = 1.1\,(\mathrm{GeV})^2)$ one gets values $\lambda = 0.38$ and 0.043, respectively, compared to the experimental values $\lambda^{\mathrm{ex}} = 0.16 \pm 0.11$ and 0.096 ± 0.013.

Forgetting about the present experimental situation, our predictions for the range of x and Q^2 where one can expect the obtained formulas to be applicable are illustrated in the table. From it one observes that the dependence on x is quite weak. In fact one obtains practically the same values of λ in the whole range $10^{-6} < x < 10^{-2}$ due to compensation of the growth with $1/x$ of both the numerator and denominator in (47). The predicted dependence on Q^2 is clearly visible, although also not very strong, which follows from (47).

4 Conclusions

Two main consequences follow for the double scattering contribution to the structure functions of the nuclei from the hard pomeron model. First, at large Q^2 it behaves as Q^{1-2x_1} where $x_1 = 0.3169$ is a number which does not depend on the coupling and so is exactly known. As a result the corresponding low-x EMC effect should go to zero as Q^{-2x_1}. This property does not seem to be changed after the inclusion of higher order rescatterings. Indeed in the dipole approach one finds that they are described by

Table 1. Predictions for the EMC ratios at large $1/x$ and Q^2

A	x	Q^2 (GeV^2)	$1 - R_{EMC}$
40	10^{-5}	10.	0.0685
		100.	0.0330
	10^{-6}	10.	0.0775
		100.	0.0374
64	10^{-5}	10.	0.104
		100.	0.0502
	10^{-6}	10.	0.118
		100.	0.0568
131	10^{-5}	10.	0.190
		100.	0.0914
	10^{-6}	10.	0.215
		100.	0.103

the pomeronic fan diagrams [12]. Then the initial pomeron coupled to the projectile will always be in the same regime as in our double scattering case with the only difference that the rest part will behave as $S^{n\Delta}$ for n rescatterings. The power $x_1^{(n)}$ governing the high Q^2 behaviour will be the smallest positive root of (32) with $2\Delta \to n\Delta$. This power grows with n: $x_1^{(3)} = 0.3793$, $x_1^{(4)} = 0.4097$, ..., $x_1^{(\infty)} = 0.5$. Contributions from higher order rescatterings will then go down at high Q^2 faster than the double scattering contribution, although by a rather small power of Q^2. Thus the behaviour $Q^{-2x_1} = Q^{-0.6338}$ seems to be a clear prediction for the small-x EMC effect which may serve to test the hard pomeron model.

Second, due to singularities at small momentum transfers, the double scattering turns out to be more strongly dependent on A as compared to the standard eikonal predictions. This second prediction does not, however, seem so trustworthy, since it relies on the specific property of the lowest order hard pomeron model of having no intrinsic scale.

References

1. S. Brodsky, T.E. Close, J.F. Gunion, Phys. Rev. **D6** (1972) 177
2. S. Brodsky, H.J. Liu, Phys. Rev. Lett. **64** (1990) 1342
3. N.N. Nikolaev, B.G. Zakharov, Z. Phys. **C49** (1991) 607
4. V. Barone, M. Genovese, N.N. Nikolaev, E. Predazzi, B.G. Zakharov, Z. Phys. **C58** (1993) 541
5. B.Z. Kopeliovich, B. Povh, Phys. Lett. **B367** (1996) 329
6. A.H. Mueller, J. Qiu, Nucl. Phys. **B268** (1986) 427
7. J. Qiu, Nucl. Phys. **B291** (1987) 746
8. E.L. Berger, J. Qiu, Phys. Lett. **B206** (1988) 141
9. N. Armesto, M.A. Braun, Z. Phys. **C76** (1997) 81
10. A. Mueller, Nucl. Phys. **B415** (1994) 373
11. J. Bartels, M. Wuesthoff, Z. Phys. **C66** (1995) 157
12. M.A. Braun, C.P. Vacca, Bologna Univ. preprint, hep-ph/9711486
13. N.N. Nikolaev, B.V. Zakharov, Z. Phys. **C64** (1994) 631
14. M. Genovese, N.N. Nikolaev, B.G. Zakharov, JETP **81** (1995) 633
15. R. Peschanski, Phys. Lett. **B409** (1997) 491
16. M.A. Braun, Z. Phys. **C71** (1996) 123
17. G.P. Korchemsky, preprint LPTHE-Orsay-97-62; hep-ph/9711277
18. A. Bialas, H. Navelet, R. Peschanski, Saclay preprints hep-ph/9711236 and hep-ph/9711442